Real-time detection of 2,4,6-trichlorophenol in environmental samples based on Fe₃O₄ nanospheres decorated graphitic carbon nitride nanosheets

Balamurugan Arumugam[a], Selvakumar Palanisamy[b*], Sayee Kannan Ramaraj[a*], Matteo Chiesa[b, c*]

[a]PG & Research Department of Chemistry, Thiagarajar College, Madurai-625009, Tamil Nadu, India.

[b]Laboratory for Energy and NanoScience (LENS), Khalifa University of Science and Technology, Masdar Campus, PO Box, 54224, Abu Dhabi, United Arab Emirates.

[c]Department of Physics and Technology, UiT The Artic University of Norway, 9010, Tromso, Norway.

*Corresponding Authors

Dr. Selvakumar Palanisamy, Email: prmselva@gmail.com; selvakumar.palanisamy@ku.ac.ae

Dr. Sayee Kannan Ramaraj, E-mail: sayeekannanramaraj@gmail.com

Prof. Matteo Chiesa, Email: matteo.chiesa@ku.ac.ae

Abstract

Real-time detection of 2,4,6-chlorophenol (TCP) has gained greater interest due to its widespread distribution and hazardous effects on living organisms. In this study, graphitic carbon nitride nanosheets decorated with Fe_3O_4 nanospheres ($CN@Fe_3O_4$) composite-modified screen-printed carbon electrodes (SPCE) were designed to develop a susceptible and selective electrochemical sensor for the detection of TCP. A compulsion method was used to synthesize CN nanosheets, and the co-precipitation method was employed to decorate the nanosheets with Fe_3O_4. The XRD confirmed a high degree of crystalline nature and exceptionally pure phase, with an average size of 38.7 nm for Fe_3O_4 on CN nanosheets. The $CN@Fe_3O_4$ composite offers a tailorable structure, fast electron transfer, and ease of preparation, making it one of the most promising electrode materials for practical applications in TCP sensing. In optimal conditions, $CN@Fe_3O_4$ modified SPCE outperformed bare, CN and Fe_3O_4 modified SPCEs to determine TCP. The analytical validations confirmed that $CN@Fe_3O_4$ modified SPCE has a linear range for TCP ranging from 0.04 to 651 μM with a detection limit of 12 nM. An assessment of the practicality of the proposed sensor in various water samples showed a recovery rate between 94.0–100.2%.

Keywords: Fe_3O_4 nanospheres; graphitic carbon nitride nanosheets; hybrid nanocomposite; 2,4,6 chlorophenol; modified screen-printed carbon electrodes; electroanalysis

1. Introduction

In recent years, real-time detection of chlorophenols and their isomers has received considerable attention due to their widespread use in agriculture and industrial processes [1]. They have also been used as an essential component for preparing pesticides, herbicides, pharmaceuticals, dyes, and disinfectants [1,2]. The 2,4,6 chlorophenol, often known as TCP, is an isomer of trichlorophenols, a class of chlorophenols used for various purposes, including the manufacturing of fungicides, herbicides, and insecticides [3, 4]. TCP has also been employed as an intermediary in various manufacturing processes, including those for creating dyes, pigments, and medications [5]. The US Environmental Protection Agency (EPA) has classified TCP as a Group 2B (probable human carcinogen) due to its neurotoxicity and latent carcinogenicity [6]. Furthermore, TCP is classified as an environmental pollutant and has been found in various freshwater lakes, including the Great Lakes in the USA [3], [4]. Corks in the wines may carry trace levels of TCP through contaminated environments from the paper pulp bleaching and wood preservative treatments using chlorinated and brominated phenols in wooden pallets and other utensils [5]. High exposure to TCP can cause an increased incidence of lymphomas, leukemia, and liver cancer in animals [6]. Therefore, reliable and precise TCP detection in environmental samples is more crucial. Due to their affordability, reaction speed, portability, and high sensitivity compared to currently available conventional analytical methods, electrochemical methods are now often utilized for the detection of TCP [7-9].

So far, different micro and nanomaterials have been successfully used for sensitive sensing of TCP [10]. In particular, the nanomaterial hybrids have been promptly used for the sensitive detection of TCP due to their high surface area and catalytic activity. For instance,

carbon nanomaterial-based hybrid nanocomposites have been widely employed for the electrochemical sensing of TCP [11-15]. Among them, graphitic carbon nitride (CN) is a class of semiconductor-based polymer type 2D material that has been widely used as promising and attractive support for stabilizing various nanomaterials and developing efficient and robust hybrid catalytic systems [16, 17]. Also, the unique physicochemical features of CN enable its widespread use in various fields, including photochemical and electrochemical sensors [18]. However, the direct use of CN in electrochemical sensing applications is limited due to its average surface area and agglomeration of the 2D nanosheet [19]. Hence, different nanomaterials such as metal oxides, metal nanoparticles, and carbon nanostructures have been engineered to improve CN's electrochemical properties and conductivity [20-23]. Recently, metal oxides have been widely used as a suitable support for the preparation of CN-based organic-inorganic hybrids, owing to their unique physicochemical properties (rapid ion diffusion pathway, larger surface-to-volume ratio, and higher storage site utilization) and applicability in various biological and industrial fields [24, 25]. Iron oxide (Fe_3O_4) is a low-cost transition metal oxide with high mobility of oxygen ions and remarkable catalytic characteristics in oxidative processes [26]. Also, it can be easily incorporated with CN and the resulting composite. It has been proven an efficient composite material for broader applications such as photocatalysis, water splitting, hydrogen production, carbon dioxide reduction, and electrochemical sensors [27-29]. The hybridization of CN with Fe_3O_4 will not only boost the accessible surface area of CN but also promote electrolyte ion diffusion, making them more favorable for the fabrication of sensitive electrochemical sensors [30].

In the current work, we have taken advantage of Fe_3O_4's unique characteristics in combination with CN to potentially boost CN's electrochemical activity and demonstrate the potential electrochemical detection of TCP. Additionally, compared to CN and Fe_3O_4-modified electrodes, the produced composite could further increase surface area, electroactive sites, and electron transfer, leading to improved catalytic activity and low-level TCA detection. For the first time, we used Fe_3O_4 nanospheres coated on CN composite-modified electrodes to create a unique TCA sensor. The sonochemical approach was employed to fabricate the $CN@Fe_3O_4$ nanocomposite, and CN nanosheets and Fe_3O_4 nanospheres were prepared through co-precipitation and compulsion methods. Compared to CN and Fe_3O_4-modified electrodes, the resulting $CN@Fe_3O_4$ composite-modified electrode exhibits good catalytic activity toward TCA. The sensor's selectivity, storage stability, and reproducibility have been studied and discussed. The practicality of the sensor for real-time detection has been demonstrated in various water samples.

2. Experimental

2.1. Chemicals and reagents

Dicyandiamide (DCN, 99%), iron (II) chloride tetrahydrate (98%), and iron (III) chloride hexahydrate (98%) were purchased from Sigma-Aldrich, India. 2,4,6-trichlorophenol, ammonium hydroxide solution (28%), sodium phosphate dibasic, and sodium phosphate monobasic were purchased from the Fluka chemicals. Screen-printed carbon electrodes (4 mm diameter) were purchased from Metrohm DropSens company. 0.05 M phosphate buffer (PB, pH 5) was used as a supporting electrolyte, and the pH was adjusted using 0.1 M NaOH and HCl.

2.2. Preparation of $CN@Fe_3O_4$ nanocomposite

CN was prepared through the calcination of dicyandiamide, as described in the literature [31]. In brief, 2.0 grams of dicyandiamide were heated at 550 °C for 4 h and cooled at room temperature using a muffle furnace at 5°C/minute. The obtained yellow powder of CN was collected and stored in an airtight container to prepare the nanocomposite. About 200 mg of as-prepared CN was dispersed in 20 mL of deionized (DI) water using a sonication method for 30 minutes. Then, 120 mg of $FeCl_2.4H_2O$ and 150 mg of $FeCl_3.6H_2O$ were added to the above-prepared CN dispersion and stirred for 20 min to attain a homogeneous suspension. After that, 10 mL of NH_4OH was rapidly added to the above suspension and stirred for 2 hours. The final product residue was centrifuged with water and ethanol several times and then dried at 60 °C overnight. The obtained product is named $CN@Fe_3O_4$ nanocomposite and is stored for further characterization and analytical studies. As mentioned above, the Fe_3O_4 nanospheres were prepared by the co-precipitation method without CN. A detailed description of the synthesis procedure for $CN@Fe_3O_4$ nanocomposite and its electrochemical applications are shown in **Scheme 1**.
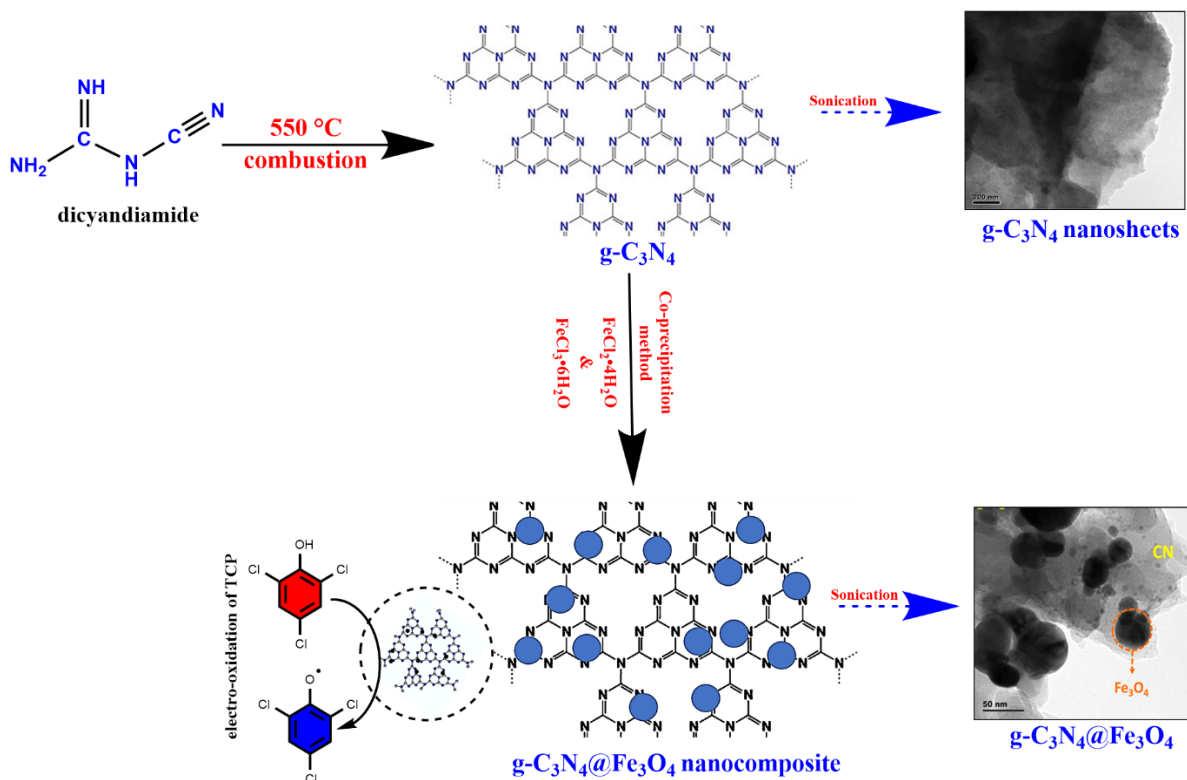
Scheme 1. Pictorial representation for the synthesis of CN@Fe$_3$O$_4$ nanocomposite and its electro-oxidation towards TCP.

2.3. Instrumentation and methods

The crystalline nature and phase purity of the as-prepared Fe$_3$O$_4$ and CN@Fe$_3$O$_4$ nanocomposite are identified by X-ray diffractometer (XRD, X'Pert PRO PANalytical BV) with Cu Kα radiation (λ = 1.541 Å). Jasco V-6600 A spectroscopy is employed to analyze Fourier transform infrared spectra within 400–4000 cm^{-1}. Thermograms are collected on TGA – 50 Shimadzu Thermogravimetric analyzer and carried under an N$_2$ atmosphere in the range of 30–900 °C. Surface and morphological analysis are identified using a high-resolution transmission electron microscope (HR-TEM, FEI TECNAI T20 G2) attached with energy dispersive X-ray (EDX) analysis.

2.4. Electrode preparation and electrochemical analysis

The unmodified SPCE was first rinsed for electrode preparation with water and ethanol to remove moisture and unreacted contaminants on its surface. In the meantime, the homogeneous suspension of the CN@Fe$_3$O$_4$ nanocomposite (5mg/mL) was prepared by dispersing the nanocomposite in DI water with sonication for 20 minutes. About 6 μL of the CN@Fe$_3$O$_4$ nanocomposite electrocatalyst was dropped onto the pre-cleaned SPCE surface. Finally, the fabricated nanocomposite-modified SPCE was dried in an air oven at 40 °C and used for electrochemical measurements. Similarly, CN/SPCE and Fe$_3$O$_4$/SPCE were prepared by drop-casting 3L of representative compounds on the surface of pre-cleaned SPCE. A CHI 660E electrochemical workstation was used for cyclic voltammetry (CV) and differential pulse voltammetry (DPV) studies with a conventional three-electrode system. The modified SPCEs were used as the working electrode, and Ag/AgCl (sat. KCl) and Pt wire were employed as the reference electrode and counter electrode, respectively.

3. Results and Discussion

3.1. Structural Characterization

The crystal nature and phase purity of Fe$_3$O$_4$ and CN@Fe$_3$O$_4$ nanocomposite are determined by XRD. In **Fig. 1A**, the XRD pattern of the Fe$_3$O$_4$ (green) was indexed to the angles of 31.3°, 35.4°, 38.7°, 48.6°, 58.1°, 61.4°, 66.2°, and 68.1°, which corresponds with the (220), (311), (400), (422), (511), (440), (531), and (620) hkl planes of the cubic inverse spinel structure of Fe$_3$O$_4$ well indexed by the JCPDS Card No: 19-0629 [32]. The CN@Fe$_3$O$_4$ nanocomposite (red) XRD pattern also shows an additional characteristic peak at 27.2°, indexed to the (002) lattice plane. This peak corresponds to the peak of carbonaceous materials resulting from in-planar stacking of

conjugated aromatic systems, confirming the presence of CN [33]. The average crystalline size of Fe_3O_4 on the nanocomposite was also calculated with the Debye-Scherer equation and found to be 38.7 nm. It is worth noting that there is a relatively more minor intensity for the CN peak than for the Fe_3O_4 significant peaks, which may be due to Fe_3O_4 preventing the interplanar stacking of CN. The XRD results confirm the presence of Fe_3O_4 and CN on the nanocomposite. In addition, FT-IR spectroscopy was used to identify the nanocomposite's functional groups and chemical compositions. The FTIR spectra of $CN@Fe_3O_4$ (red) and pure Fe_3O_4 (green) are shown in **Fig. 1B**. As can be seen that the broad peak observed between 3100 and 3380 cm^{-1} is attributed to the stretching vibration of the -OH group of H_2O. The sharp peak at 542 cm^{-1} is associated with the Fe-O stretching vibration of Fe_3O_4. The $CN@Fe_3O_4$ (red) shows a broad peak at 3200 cm^{-1} assigned to the N–H stretching vibration. The firm absorption peaks observed from 1160 to 1600 cm^{-1} ascribed to the characteristic stretching vibrations of C–N heterocycles of tri-s-triazine. The peak at 865 cm^{-1} is attributed to the breathing mode of triazine ring vibrations, which depict the ordered heptazine with deprotonation. The peaks at 537 cm^{-1} are attributed to the Fe-O stretching vibration, which confirms the presence of Fe_3O_4. The obtained results include all distinct peaks of CN and Fe_3O_4, which supports the successful synthesis of the $CN@Fe_3O_4$ nanocomposite.
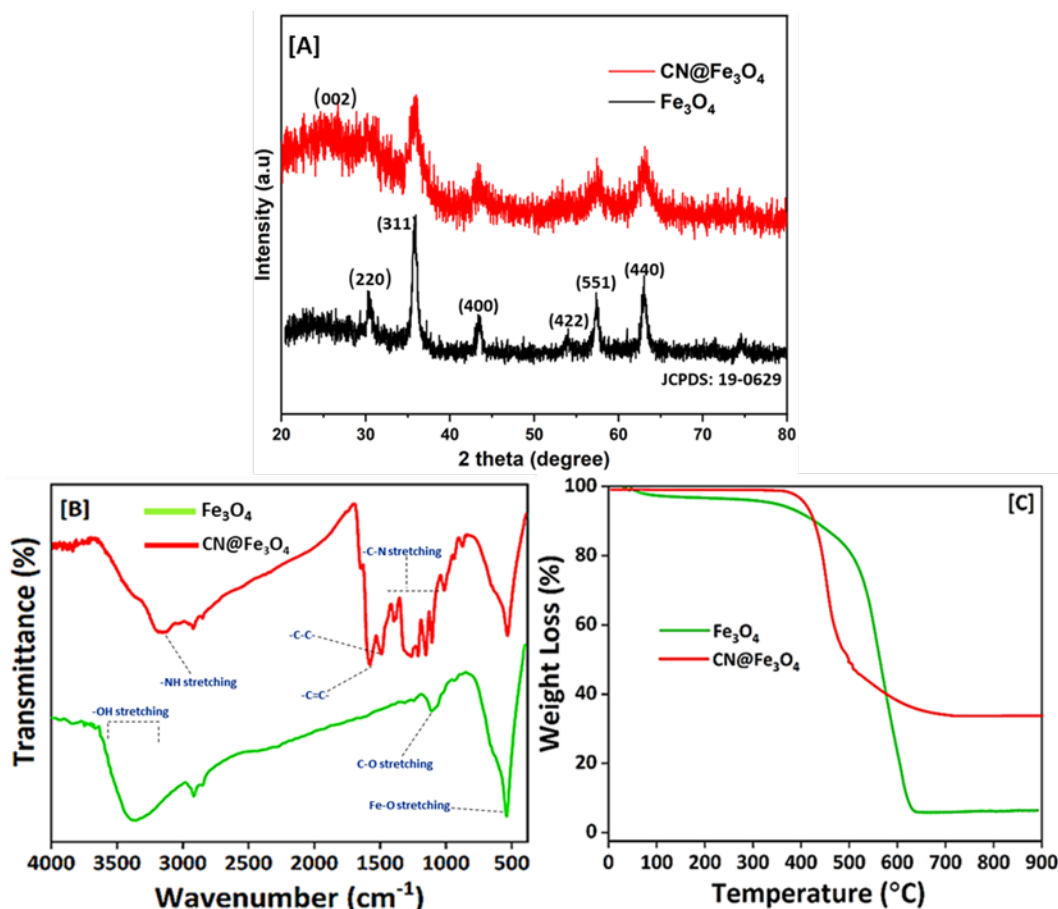
Figure 1. [A] XRD pattern [B] FT-IR spectrum and [C] TGA analysis of Fe_3O_4 and $CN@Fe_3O_4$ nanocomposite.

The thermal stability of the as-prepared Fe_3O_4 and $CN@Fe_3O_4$ nanocomposite was examined by TGA analysis, and their corresponding weight loss is depicted in **Fig. 1C**. A gradual loss of weight from 80 to 300 °C is caused by chemically adsorbed water molecules in Fe_3O_4. A second weight loss from 600 to 675 °C results from the conversion of Fe_3O_4 to α-Fe_2O_3. Due to the sublimation or decomposition of CN, the nanocomposite experiences its first weight loss between 430 °C and 600 °C. These results indicate that CN exists in the nanocomposite, slightly reducing its stability. There was no change in subsequent treatments, reinforcing the tenacious structure of the $CN@Fe_3O_4$ nanocomposite containing 93.6% Fe_3O_4 and 6.4% CN.

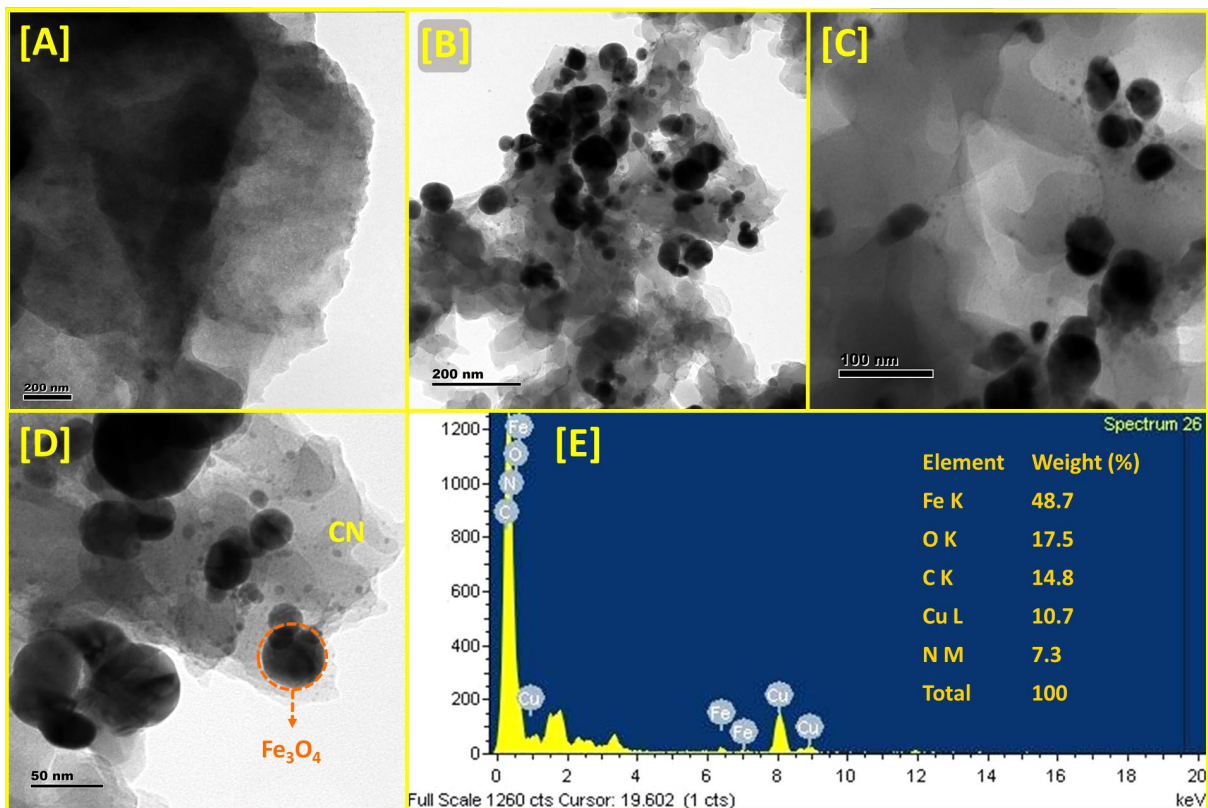**Figure 2.** HR-TEM images of CN [A] and CN@Fe_3O_4 nanocomposite in different magnifications [B-D]. [E] The corresponding EDX analysis of the CN@Fe_3O_4 nanocomposite.

As-prepared Fe_3O_4 and CN@Fe_3O_4 nanocomposite structures and morphological features were analyzed using HR-TEM and EDX, and the results are presented in **Fig. 2**. According to **Fig. 2A**, the CN has a nanosheet-like morphology, with layers stacked on top of each other. Low-resolution HR-TEM images of the CN@Fe_3O_4 nanocomposite shown in Fig. 2B and C indicate that the Fe_3O_4 has a nanosphere-like morphology and is well decorated on the surface of CN. The average diameter of Fe_3O_4 nanospheres was 43 nm (**Fig. 2D**) on the nanocomposite, consistent with the XRD results. This construction allows it to incorporate each component's advantages, including a large active area and excellent electronic transfer. Synergistic binding and interpretation of the active sites are achieved by the synchronized contribution of Fe_3O_4 and CN

in the nanocomposite. As a result, the diffusion pathway for ions condenses electrical conductivity, increasing electron/ion transport. The EDX profile for nanocomposite results is shown in **Fig. 2E**. According to the EDX spectrum, Fe, O, C, N, and Cu have weight percentages of 48.7, 17.5, 14.8, 7.3, and 10.7, respectively. The obtained results confirm the successful formation of the $CN@Fe_3O_4$ nanocomposite.

3.2. Electrochemical measurements

The electrochemical detection of bare SPCE, Fe_3O_4/SPCE, and $CN@Fe_3O_4$/SPCE is performed with CV in the presence of 200 μM TCP in pH 5.0 at 50 mV/s scan rate. According to Fig. 3A, the bare SPCE has a poor voltammetric response towards the oxidation of TCP, revealing a slow electron transfer process and catalytic behavior. In the Fe_3O_4/SPCE system, an oxidation current of 6.8 A was observed at a potential of 0.83 V. In contrast, a slight difference in peak potential 0.827 V was observed for the $CN@Fe_3O_4$/SPCE, indicating improved electrocatalytic oxidation of TCP. There are two critical reasons for this: large surface area, rich active sites, p-p conjugation, and effective conductivity of CN, which result in a different connection between TCP and $CN@Fe_3O_4$/SPCE interfaces. In addition, $CN@Fe_3O_4$-modified electrodes have oxygen atoms and functional groups that directly interact with TCP. By combining metal oxide and carbonaceous materials with specific properties, different nanosized materials enhance the electrochemical properties of TCP detection. Additionally, the TCP predominantly oxidized into phenoxy radicals in this electrochemical oxidation reaction, as shown in **Scheme 1**. Further examination of $CN@Fe_3O_4$/SPCE for catalytic activity with CV in the presence of varying concentrations of TCP from 50 to 300 μM. The experiments were performed in 0.05 M PB electrolyte (pH 5.0) at a 50 mV/s scan rate, and the obtained CV peak responses are displayed in

Fig. 3B. Furthermore, the anodic oxidation current grows with increasing TCP concentration, ranging from 50 to 300 μM, demonstrating the superior electro-oxidation behavior of CN@Fe$_3$O$_4$/SPCE which is due to the larger active surface area and the combination of Fe$_3$O$_4$ decoration on the CN surface. In addition, **Fig. 3C** illustrates the linear relationship between anodic oxidation and TCP concentration. This indicates that the oxidation peak response has improved swiftly without a shift in peak potential, confirming that the CN@Fe$_3$O$_4$/SPCE has excellent catalytic performance for TCP detection based on the linear fitting equation (I_{pa} = 0.0325 + 2.2319) and correlation coefficient (R^2 = 0.9917). The log TCP concentration versus log oxidation current plot in Fig. 3D was used to evaluate the kinetics of the TCP process in CN@Fe$_3$O$_4$/SPCE. According to the linear fitting equation I_{pa} = 0.6546 − 0.5667 with R^2 = 0.9948, the slope value is near 1, indicating that the electrocatalytic oxidation of TCP at CN@Fe$_3$O$_4$/SPCE is governed by first-order rate kinetics.

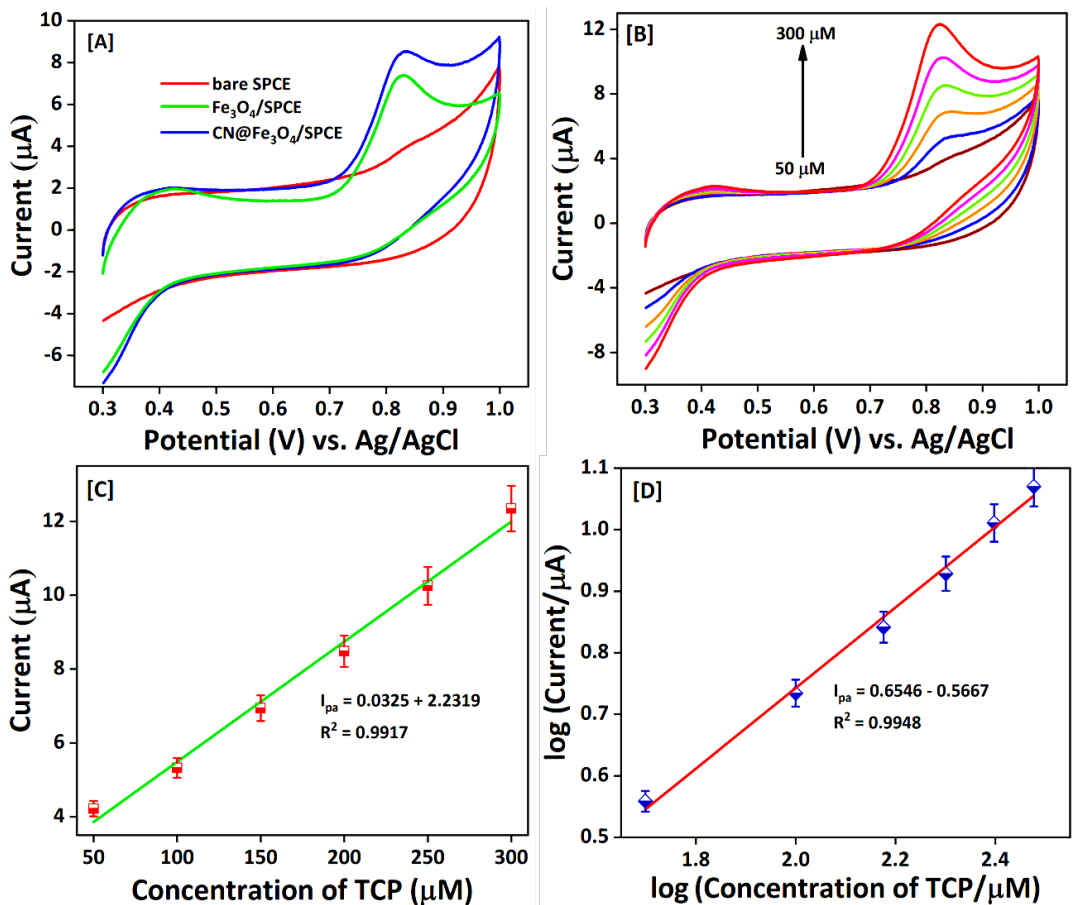**Figure 3.** A] CVs of bare SPCE, Fe_3O_4/SPCE, and CN@Fe_3O_4/SPCE in the presence of 200 μM TCP, [B] CVs of CN@Fe_3O_4/SPCE with different concentrations of TCP from 50 to 300 μM in 0.05M PB solution electrolyte (pH 5.0) at 50 mV/s scan rate, [C] Linear Fitting plot of concentration of TCP against peak oxidation current, [D] Linear fitting plot for the logarithmic concentration of TCP vs. logarithmic peak oxidation current.

3.3. Effect of Scan Rate and pH

During the determination of TCP, the scan rate significantly influenced the charge transfer performance and electrocatalytic reaction mechanism of the modified electrode. The influence of the scan rate on the CN@Fe_3O_4/SPCE was studied by differentiating the scan rate from 20 to

200 mV/s in 200 μM TCP containing pH 5.0. **Fig. 4A** shows that the oxidation peak current of TCP

grew gradually in response to increasing scan rate with positive potential shift, suggesting that

the scan rate directly affected TCP's superior electrochemical performance. According to **Fig. 4B**,

the linear fit of the scan rate versus peak current is I_{pa} = 0.0902 + 5.5297 with R^2 = 0.9963,

indicating that the anodic peak current is directly proportional to the scan rate. Fig. 4C of the

calibration plot shows that the oxidation current of TCP had a linear dependence with the square

root of scan from 20 to 200 mV/s, and the corresponding regression equation can be written as

I_{pa} = 1.7372 − 1.9773 and R^2 = 0.9931. The results indicate that the electrocatalytic oxidation of

TCP on CN@Fe$_3$O$_4$/SPCE is a diffusion-controlled electrochemical process. To further confirm this

phenomenon, the logarithmic scan rate vs. logarithmic peak current was plotted, and the

calibration plot is displayed in Fig. 4D. The corresponding regression equation was written as I_{pa}

= 0.5420 + 0.101 with the coefficient of R^2 = 0.9926. Notably, the slope value of 0.5420 is close

to the reported theoretical value of 0.5 for a pure diffusion-controlled electrochemical system;

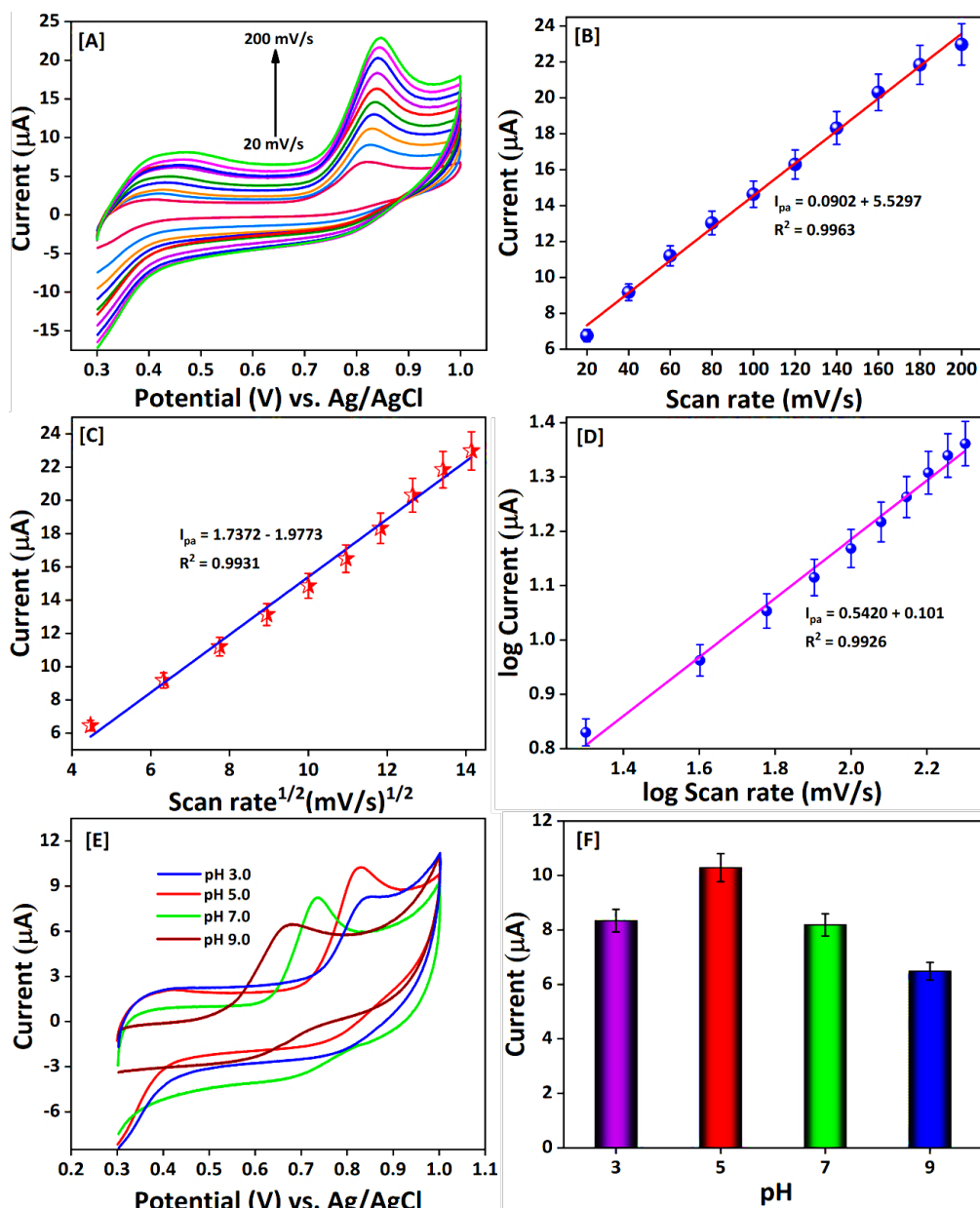hence, the catalysis of TCP is a pure diffusion-controlled process on the modified electrode.

Figure. 4 [A] CVs of 100 µM TCP at CN@Fe$_3$O$_4$/SPCE with varying scan rates from 20 to 200mV/s in 0.05 M PB electrolyte solution (pH 5.0), [B, C] Calibration plot of scan rate vs. peak current and the square root of scan rate vs. peak current, [D] Linear plot of logarithmic of scan rate vs. logarithmic peak current. E] CVs of CN@Fe$_3$O$_4$/SPCE in the presence of 250 µM TCP with diverse pH values 3.0, 5.0, 7.0, 9.0, in 0.05 M PB electrolyte and [F] is the corresponding bar diagram for pH vs. oxidation current response.

It is important to note that the pH of the electrolyte plays a crucial role in the electrochemical determination of TCP since it can easily affect the peak potential and the peak current of TCP. Hence, the CV response of CN@Fe$_3$O$_4$/SPCE was studied in the presence of 250 μM TCP containing various pHs from 3.0 to 9.0. **Fig. 4E** shows that the anodic peak current response of TCP was raised when the pH was increased from 3.0 to 5.0. At the same time, the current response decreased upon increasing the pH from 5.0 to 9.0. The corresponding bar diagram for the relationship between pH vs. peak current is displayed in Fig. 4F. Nevertheless, the peak potential decreased from 5.0 to 9.0, which is attributed to the presence of protic aromatic isomer units on TCP. In response to higher pH values, these aromatic molecules undergo deprotonation and become anions, causing electrostatic repulsion between TCP and CN@Fe$_3$O$_4$/SPCE, causing the peak current to decline. The maximum anodic current response was attained at pH 5.0, which led to the transformations of an isomer of phenoxy radicals, finally giving the oxidized product of TCP. Hence pH 5.0 was chosen as the optimized electrolyte solution pH for all the electrochemical investigations of the TCP sensor using CN@Fe$_3$O$_4$/SPCE.

3.4. Electrocatalytic Determination of TCP

We used DPV to estimate the dynamic response range, the detection limit, and the sensitivity of the proposed CN@Fe$_3$O$_4$/SPCE for determining TCP. **Fig. 7A** illustrates the DPV responses of CN@Fe$_3$O$_4$/SPCE toward different concentrations of TCB in pH 5 with a 0.05 V amplitude. When DPV is optimized without TCB, CN@Fe$_3$O$_4$/SPCE shows no obvious DPV response (curve not shown). DPV response was sharp and stable for TCP additions of 0.04 μM, and the oxidation peak current increased for TCP at the modified electrode with an increase in

TCB concentration between 0.04 μM to 651 μM. Sensor response time (the time it took for 91% of the steady current to reach 90% current response) was calculated as 7 s, which indicates that CN@Fe$_3$O$_4$/SPCE has excellent catalytic activity against TCP. The oxidation peak current of TCP linearly increases over TCP concentrations ranging from 0.04 μM to 651 μM (Fig. 7B). This calibration plot illustrates the broad dynamic response range with a linear regression equation 0.0202x + 1.1982 with correlation coefficient R^2 = 0.9983. The sensitivity for electrochemical oxidation of TCP was calculated from the slope of the calibration plot and the surface area of the electrodes. We determined the detection limit of the sensor (LOD) based on 3σ/S, where S represents the slope of the calibration plot, and σ represents the standard deviation (S/N = 3). The LOD and sensitivity of the developed sensor were calculated as 12 nM and 0.0202 μAμM^{-1}, respectively. LOD and sensitivity were more comparable than those previously reported for the electrochemical detection of TCP. In particular, our sensor has a lower LOD than previously reported graphene, carbon nanotubes, and other carbon nanomaterial composite sensors. Based on the sensitivity and LOD of the CN@Fe$_3$O$_4$ composite modified electrode, it is evident that it exhibits better analytical performance toward TCP than the earlier described modified electrodes. As a result of the combination of unique properties of CN and Fe$_3$O$_4$ in the composite, the sensor electrode exhibits excellent electrocatalytic activity, which increases its electrocatalytic activity for TCP and prevents the fouling of oxidized products.
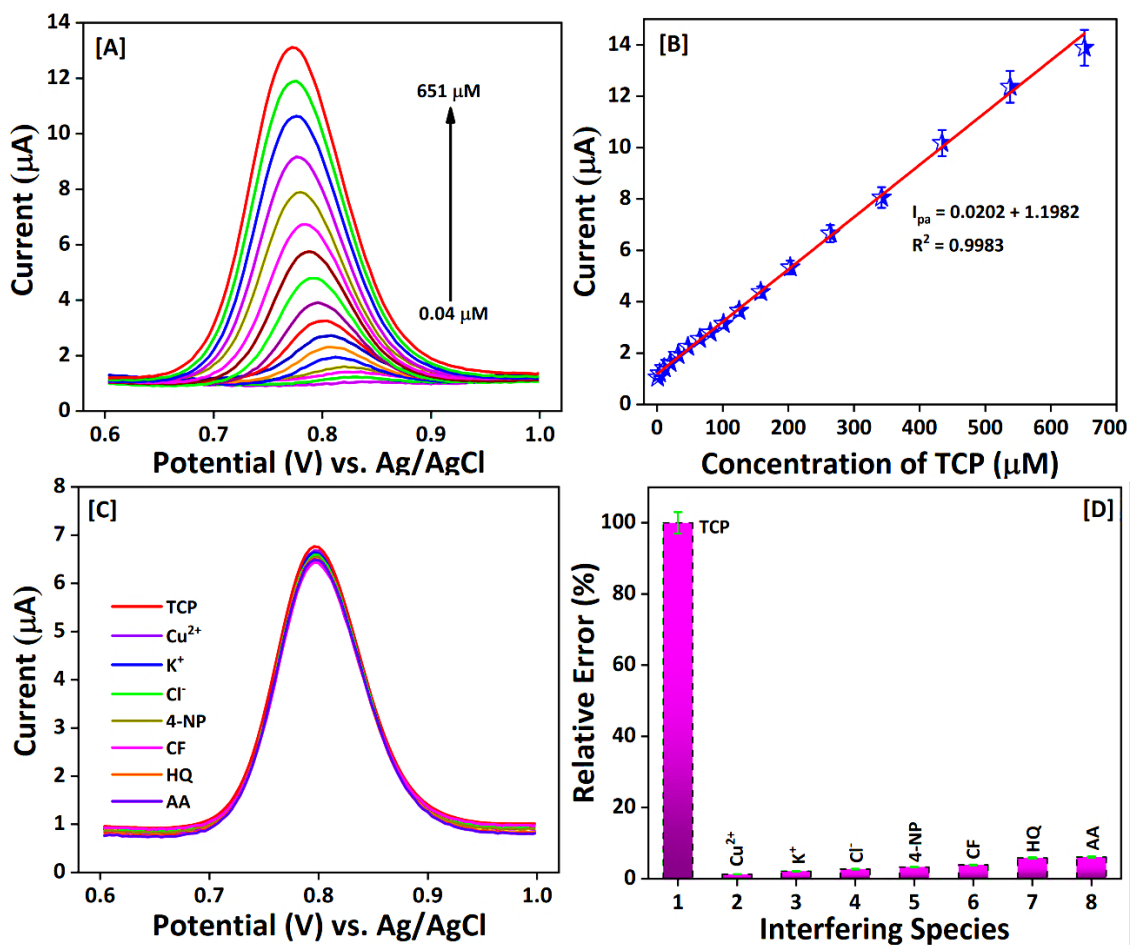
Figure. 5 [A] DPV oxidation peak responses of CN@Fe$_3$O$_4$/SPCE with various concentrations of TCP 0.04 to 651 μM in 0.05 M PB electrolyte (pH 5.0), [B] Dependence linear plot for concentration of TCP vs. oxidation peak current, [C] DPV responses at CN@Fe$_3$O$_4$/SPCE in the presence of 200 μM TCP with the 20-fold excess concentration of Cu^{2+}, K$^+$, Cl$^-$, 4-nitrophenol (4-NP), carbofuran (CF), hydroquinone (HQ), and ascorbic Acid (AA), [D] Corresponding relative error (%) vs. TCP and interfering species.

3.5. Selectivity, reproducibility, and storage stability of the CN@Fe$_3$O$_4$ modified SPCE

It is more critical to demonstrate the selectivity of the modified electrode for future practical applications. A DPV was used for testing the selectivity of the CN@Fe$_3$O$_4$/SPCE for TCP

detection in the presence of various potentially interfering electroactive compounds. **Fig. 5C** exhibits the DPV response of CN@Fe$_3$O$_4$/SPCE for the presence of 200 μM TCP with the 20-fold excess concentration of Cu^{2+}, K$^+$, Cl$^-$, 4-nitrophenol (4-NP), carbofuran (CF), hydroquinone (HQ), and ascorbic acid (AA). Interestingly, the interfering compounds did not affect the TCP peak response, and the oxidation peak response of TCP was also unchanged. However, 4-NP, CF, HQ, and AA show little effect on the sensor electrode, yet it is not imperative compared to the response of TCP on the modified electrode surface. The corresponding selectivity bar chart is shown in **Fig. 5D**. It is evident that the CN@Fe$_3$O$_4$/SPCE has high selectivity towards the detection of TCP in the presence of various metal ions phenolic compounds. Additionally, storage stability and reproducibility of CN@Fe$_3$O$_4$/SPCE were studied to prove the practical viability of the TCP sensor. DPV was used to study the storage stability and reproducibility of the sensor. **Fig. 6A** shows the storage stability analysis of the CN@Fe$_3$O$_4$/SPCE for detecting 200 μM TCP on a different day in travels up to 20 days by DPV. If the modified electrode was not in use, it was stored in an airtight vial at room temperature in dry conditions. It can be seen that there is only a slight change in the oxidation current response of TCP on the modified electrode. It conquers 98.6% of its initial peak current after 20 days revealing the outstanding storage stability of the CN@Fe$_3$O$_4$ fabricated sensor. Three individual CN@Fe$_3$O$_4$/SPCEs were fabricated and scrutinized in pH containing TCP (200 μM) within the potential range of 0.6 to 1.0 V. The observed DPV results for reproducibility analysis are displayed in **Fig. 6B**. In the detection of TCP, the relative standard deviation of CN@Fe$_3$O$_4$/SPCE was calculated to be 4.16%, indicating that the electrode can be reproduced with appropriate reproducibility.
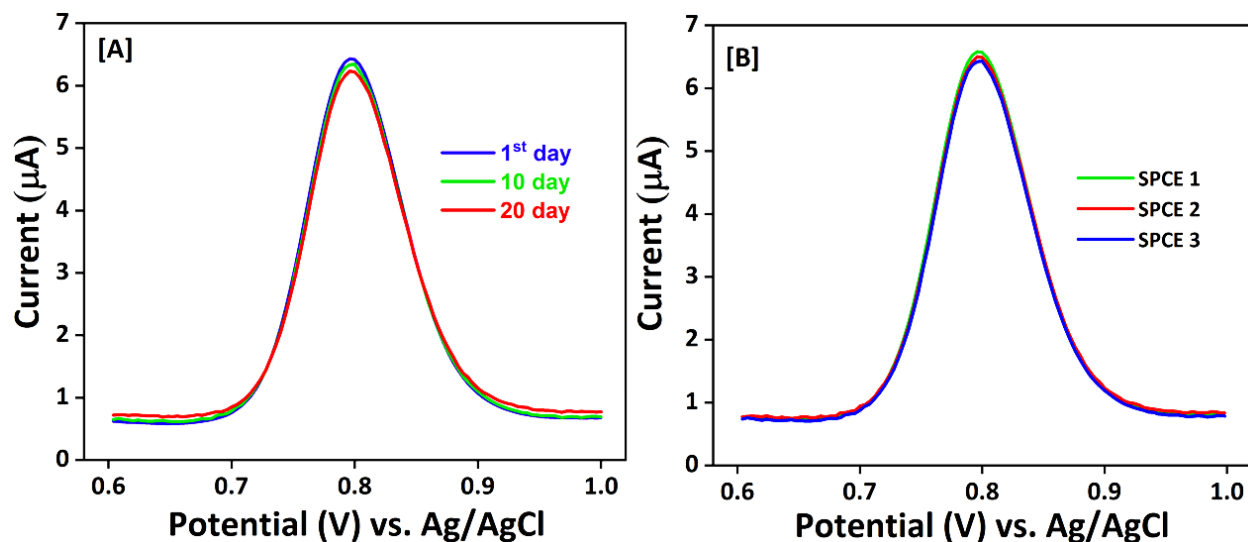
Figure 6 [A] & [B] Storage stability and reproducibility of the CN@Fe$_3$O$_4$/SPCE with the presence of 200 μM TCP in 0.05 M PB electrolyte (pH 5.0).

3.5. Practicality of the sensor electrode

TCP containing various water samples was analyzed using the standard addition method to determine the practical suitability of the modified electrode. The tap water and drinking water samples were collected from the inside campus of Thiagarajar College, Madurai, and were not purified or modified. Samples of river water were collected near Thiagarajar college from the Vaigai river. A Whatman Filter Paper (grade 1) was used to filter the river water sample before it was used for real sample analysis. These water samples were analyzed using DPV and were found to be TCP-free. Different concentrations of TCP were added to drinking, river, and tap water samples and were analyzed by DPV. A summary of the recovered results of TCP is shown in **Table T1**. Based on actual sample data, CN@Fe$_3$O$_4$/SPCE displays excellent recovery towards TCP (94.0–100.2%). The results prove the feasibility of the proposed TCP sensor and indicate that it could be used for measuring TCP directly in environmental samples.

Table 2. The practicality of CN@Fe$_3$O$_4$/SPCE for determining TCP in different water samples.

Real sample	Added (μM)	Found (μM)	*Recovery (%)
Tap water	0.5	0.49	98.0
	5	4.92	98.4
	20	19.87	99.4
Drinking water	0.5	0.49	98.0
	5	4.95	99.0
	20	20.03	100.2
River water	0.5	0.47	94.0
	5	4.78	95.6
	20	19.71	98.6

* indicates that the recoveries were calculated using the standard addition method.

4. Conclusion

In summary, CN@Fe$_3$O$_4$/SPCE-based sensor was fabricated for the real-time detection of TCP for the first time. The as-prepared nanocomposite materials were primarily evaluated and confirmed using XRD, FT-IR, TGA, HR-TEM, and EDX analysis. The CN@Fe$_3$O$_4$ nanocomposite-modified electrodes have advantages: enlarged active surface area, outstanding electron transport properties, trace-level detection with high sensitivity, and quick response. The CN@Fe$_3$O$_4$ modified SPCE has a detection limit of 0.016 μM and a wide dynamic (up to 651 μM) for the determination of TCP. In addition to that, the proposed sensor encompasses outstanding

sensitivity, selectivity, reproducibility, and storage stability properties. Based on the results obtained above, we can conclude that CN@Fe$_3$O$_4$ can detect TCP in the future and for energy-related devices and photocatalytic applications.

5. Declaration of Competing Interest

The authors declare that they have no known competing financial interests or personal relationships that could have appeared to influence the work reported in this paper.

References